Fracture 1977, Volume 3, ICF4, Waterloo, Canada, June 19 - 24, 1977

CRACK PROPAGATION INITIATION IN DUCTILE STRUCTURES

J. Lebey and R. Roche*

INTRODUCTION

Linear Elastic Fracture Mechanics is now well established. The determination of K_I is a simple mathematical problem, and the methods for determining its critical value are well known. LEFM can only be applied in cases where inelastic strain (plasticity, creep) is strictly localized. In actual practice, fractures of mechanical parts are preceded by significant plastic strains. In such cases, LEFM is incapable of clarifying the fracture conditions [1] [2] [3]. Initiation of the propagation of an existing crack occurs at loads lower than those specified by LEFM. This is especially true for ductile metallic materials such as standard structural steels.

This points to a pressing need for the development of Post Yield Fracture Mechanics, for a better knowledge and prediction of fracture conditions governing a large number of structures. In this area, a number of criteria have already been proposed. The best known are the Crack Opening Displacement and the J integral [4] [5] [6]. However, it is always difficult to substantiate the validity of a criterion, and the latter, like many others, have been subject to debate. Hence it appears indispensable to increase the number of experimental results which can help to define the field of application of any specific criterion. It is with this in mind that the Research Centre at Saclay undertook a programme concerned with thin structures of structural elements, in which crack propagation initiation occurs with substantial plastic strain. This paper gives the results obtained with two types of structures:

(a) centre cracked plates from a single steel previously subjected to various degrees of strain hardening,

(b) spheres of different dimensions.

CENTRE CRACKED PLATES

The plates, the dimensions of which are given in Figure 1, were machined from XC10 steel† 8 mm thick. After measurement of the mechanical properties of the metal as received, a number of rough test pieces were cold worked before final machining.

The cold working process involved elongation of the metal by longitudinal tension (previous elongation PE).

The initial elongation obtained is expressed as a percentage of the proportional elongation A_p at maximum load of the metal as received.

*Centre d'Etudes Nucléaires de Saclay, France.
†Composition : C 0.10; Mn 0.40; Si 0.25; S + P < 0.035

Three previous elongations were adopted : 20%, 50% and 80% of A_p.

With the non cold worked metal (as received), this provided four different groups of mechanical properties, as shown in Table 1.

The initial length $2a_o$ of the notches ranged from 5 to 50 mm; the end radius of the notch, obtained by electro-erosion, was 0.5 mm, with fatigue pre-cracks.

During the tests, the stress and displacement at the centre of the notch were recorded on an XY recorder. The crack initiation at the notch end was observed visually by means of a binocular microscope.

The results given in Table 2 are concerned exclusively with crack initiation conditions, in which :

$$\sigma_i \text{ net} = \frac{\text{load at initiation}}{(W-2a_o) \times \text{thickness}}$$

$$\sigma_i \text{ gross} = \frac{\text{load at initiation}}{W \times \text{thickness}}$$

Δ_{li} = variation in central opening at initiation

J_{Ic} = critical value of the J integral, measured by the method indicated in [7].

The recordings obtained did not enable the measurement of J_{Ic} in cases of previous elongation 50% and 80%.

The different results are presented in graphic form in Figures 2, 3, 4 and 5.

Figure 2 shows that, in all cases, the yield stress must be reached on the remaining ligament for crack initiation to occur; no embrittlement occurs due to strain hardening. In all cases, the cracks were subsequently propagated in a stable manner.

Figure 4 shows that the critical value of the central opening depends on the state of strain hardening of the metal.

The determination of J_{Ic} is complicated by the need to derive the experimental results. The results obtained do not make it possible to confirm that the criterion is adequately substantiated for a ductile material in the probable case of plane stresses.

SPHERES

Tests were performed on manganese-molybdenum steel spheres of three different dimensions :

5 spheres diameter D 363 mm thick e 3 mm
2 spheres diameter D 918 mm thick e 7 mm
3 spheres diameter D 1800mm thick e 15mm
} theoretical dimensions

The spheres featured thru notches terminated by radii of about 0.1 mm, with fatigue pre-crack.

The experimental method is described in previous publications [8] [9] [10], together with part of the results, obtained previously.

The mechanical properties and test results are given in Tables 3 and 4, in which the stresses indicated as σ_i and σ_p are respectively :

σ_i crack initiation stress

σ_p unstable crack propagation stress

Two crack propagation modes were observed, depending on the test; they are illustrated by the R curves in Figure 6 concerning 1800 mm diameter spheres.

(a) stable propagation from the initiation stress σ_i to the unstable propagation stress σ_p, at which the crack propagates rapidly at constant pressure. This type of fracture was observed in all tests on spheres 363 and 918 mm in diameter, and with the 1800 mm diameter No. 3, it corresponds to ductile tears.

(b) sudden fracture without stable propagation period; in this case, σ_i and σ_p coincide; this fracture mode was observed with 1800 mm diameter spheres, Nos. 1 and 2.

These results highlight the effect of the scale factor, already investigated elsewhere [11], on the strength of cracked vessels. The initiation stress values, related to the yield stress of the metal, are indicated in Figure 7 as a function of the relative length of the initial notch. Figure 8 shows the appearance of sphere No. 2 after sudden fracture.

In view of the thin dimensions, it proved impossible to take valid measurements of toughness (K_{Ic}) by standard methods [12]. However, an estimate of toughness can be made by using the method of equivalent energy (K_{Icd}) [13] or by measuring J_{Ic} experimentally by two different methods [7], [14], and by calculating K_{Ic} with the values thus obtained. This enables calculation of the theoretical crack initiation stresses, for comparison with the experimental values. Table 5 shows a number of these comparisons drawn up by calculating the initiation stresses from toughness measurements taken with CT specimens taken from spheres (and of substantially identical thickness to that of the spheres). The σ_i values calculated were obtained as follows :

$$\text{column A : } \sigma_i = \frac{K_{Icd}}{\alpha\sqrt{\pi a}}$$

$$\text{column B : } \sigma_i = \frac{\sqrt{J_{Ic} \cdot E}}{\alpha\sqrt{\pi a}} \quad \text{with } J_I = \frac{2U}{A} \quad [14]$$

$$\text{column C : } \sigma_i = \frac{\sqrt{J_{Ic} \cdot E}}{\alpha\sqrt{\pi a}} \quad \text{with } J_I = -\frac{dU}{da} \quad [7]$$

where : $\alpha = \sqrt{1 + \frac{1.9a^2}{R.\ e}}$ (Folias)

with R = radius of sphere
e = thickness of sphere

CONCLUSIONS

The results obtained are only applicable to a limited area; however, it nevertheless appears clear that it is not possible to exceed the generalized plasticity load without this resulting at least in stable propagation of existing cracks. In most cases stable propagation occurs before reaching generalized plasticity, but it seems possible, by using criteria of the equivalent energy or J_{Ic}, to predict with reasonable accuracy the load which causes propagation initiation [15]. Note that in all cases the thicknesses were too low for a valid measurement of K_{Ic}. While one cannot draw a general conclusion from the foregoing, it appears in the present case that propagation initiation occurs at the lower of the two following loads :

(a) limit loading

(b) loading calculated by means of a criterion of the J integral or equivalent energy type.

ACKNOWLEDGEMENTS

This study was sponsored by the Nuclear Safety Delegation of the CEA. The authors wish to thank those members of the Nuclear Safety Department who provided them with assistance.

REFERENCES

1. HAHN, G. T., SARRATE. M. and ROSENFIELD, R., Int. Journal of Fracture Mechanics S. 1969.
2. EIBER, R. J., MAXEY, W. A. and DUFFY, A. R., Rapport BMI 1883, 1970.
3. HEALD, P. T., SPINK, G. M. and WORTHINGTON, P. J., Materials Science Eng. 10, 1972.
4. NICHOLS, R. W., BURDEKIN, G. M., COWAN, A., ELLIOTT, D. and INGHAM, T., Symposium on Fracture Toughness Concepts for Weldable Structural Steels, I.I.W., IX 655-69 X-534-69.
5. RICE, J. R., in Fracture, Academic Press, 1968, 191.
6. RICE, J. R., Journal of Appl. Mech., June 1968.
7. LANDES, J. D. and BEGLEY, J. A., ASTM STP 514, 1972.
8. DORE, A., FOGLIA, S., LEBEY, J. and TOMACHEVSKY, E., Second Int. Conf. on Structural Mechanics in Reactor Technology, Berlin, 1973.
9. FOGLIA, S., LEBEY, J. and ROCHE, R., National Conf. on Technology in Pressure Vessels, Paris, 1975.
10. LEBEY, J. and ROCHE, R., Third Int. Conf. on Structural Mechanics in Reactor Technology, London, 1975.
11. DOWLING, A. R., Rapport CEGB RD/B/N 2796, October 1973.
12. ASTM Part 31, 1970.
13. WITT, F. J., 4th National Symposium on Fracture Mechanics, Pittsburg, 1971.

14. RICE, J. R., PARIS, P. C. and MERKLE, J. G., ASTM STP 536.
15. NEALE, B. K. and TOWNLEY, C. H., Rapport C.E.G.B. RD/B/N 3358, May 1975.

Table 1 Center Cracked Plates. Mechanical Characteristics

Previous Elongation (P.E.)	Yield Strength σ_y 0,2 (hb)	U.T.S. σ_R (hb)	% Elongation at Maximum Load	% Elongation at Failure	Strain Hardening Exponent
As received	28,5	42	23	40	0,20
20%	38	46	10	20	0,095
50%	48	51	5,5	16	0,053
80%	53	54	3	13	0,029

Table 2 Center Cracked Plates. Test Results at Initiation

Specimen n°	$2a_o$ (mm)	Thickness (mm)	Previous Elongation	σ_i Net (hb)	σ_i Gross (hb)	Δ_{li} (mm)	J_{Ic} (J/mm²)
16	5	3	As received	37,1	35,5	1,44	
9	10	3		31	28,4	1,60	
10	20	3		31,2	26	1,10	0,22
11	30	3		31,1	23,3	1,35	0,27
13	40	3		31,5	21	1,12	0,23
14	40	6		33,4	22,2	1,6	0,31
12	50	3		32,2	18,8	1,7	0,33
15	50	6		32,6	19	1,54	0,30
7	10	3	20%	41,5	38	1	0,17
8	50	3		43,4	25,3	1,18	0,206
5	10	3	50%	49,5	45,3	0,40	
6	50	3		51	29,8		
2	10	3	80%	54,4	49,8		
3	10	3		54,5	50	0,16	
4	50	3		54,5	31,9		

Table 3 Spheres. Mechanical Characteristics and Test Results

D (mm)	Sphere n°	Mechanical Characteristics σ_y 0,2 (hb)	σ_R (hb)	e (mm)	2a (mm)	P (bars) P_i	P_p	(hb) σ_i	σ_p
363	9			2,45	35	90	98	33	36,2
				2,25	70	51	63	20,5	25,5
				2,20	105	32	42	13,2	17,3
	10	36,2	51,8	2,70	40	95	99	31,8	33,2
				2,70	59	60	68	20	22,8
	13	36,2	52,5	2,15	35	80	84	33,6	36,2
				2,35	50	66	76	25,4	29,2
				2,50	65	60	72	21,7	26
				2,52	72	50	65	18	23,6
				2,50	80	46	56	16,6	20,5
				2,20	95	32		13,2	
				2,10	102	29		12,5	
				2,20	110	28	37	11,5	15,4
				2,35	125	26	33	10	12,7
	15	39,7	52,5	2,17	15	88	86	36,8	41,5
				2,12	25	99	92	36,8	39,5
	19	36,4	52	2,45	56	55	76	20,3	28
				2,80	61	63	73	20,4	23,5
				2,55	75	52	63	18,5	22,5
				2,80	99	35	50	11,3	15,5

Table 4 Spheres. Mechanical Characteristics and Test Results

D (mm)	Sphere n°	Mechanical Characteristics σ_y 0,2 (hb)	σ_R (hb)	e (mm)	2a (mm)	P (bars) P_i	P_p	(hb) σ_i	σ_p
	1	28	48,5	4,70	110	50	56	24	27
				4,75	140	38	50	18,3	23,8
				4,90	170	33	46	15,6	21,6
				4,70	205	25	37	12	18,1
				5	230	24	38	11	17,5
				4,75	260	22	33	10,2	16
				4,90	318	16	30	7,5	13,8
1800	2	27,1	48,8	4,65	173	32	41	15,5	20,3
	1	50,5	65,7	14	400	32	32	10,4	10,4
	2	50	68	14	300	48	48	15,2	15,2
	3	50	69,5	14	550	19	40	6	12,8

Table 5 Spheres. Calculated and Experimental Stress σ_i for Initiation of Crack

D (mm)	Sphere n°	$2a_o/D$	σ_i calculated (hb) (A)	(B)	(C)	σ_i Experimental (hb)	Propagation
363	13	from 0,090	54,6			33,6	Stable
		to 0,345	10,6			10	
1800	2	0,167	11	13,6	12,4	15,2	Unstable
	1	0,222	8,1			10,4	Unstable
	3	0,305	5,4	5,9	5,69	6	Stable

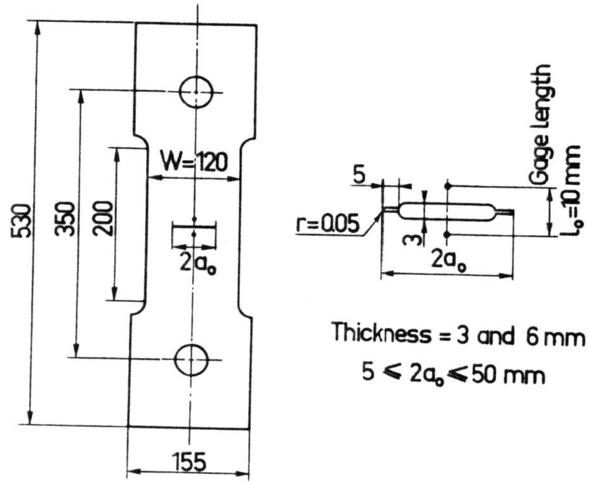

Figure 1 Center Cracked Plates Dimensions

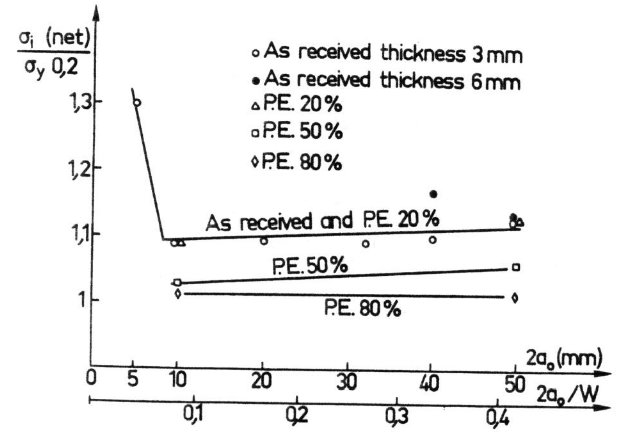

Figure 2 Center Cracked Plates. Relation Between the Net Initiation Stress and the Crack Length

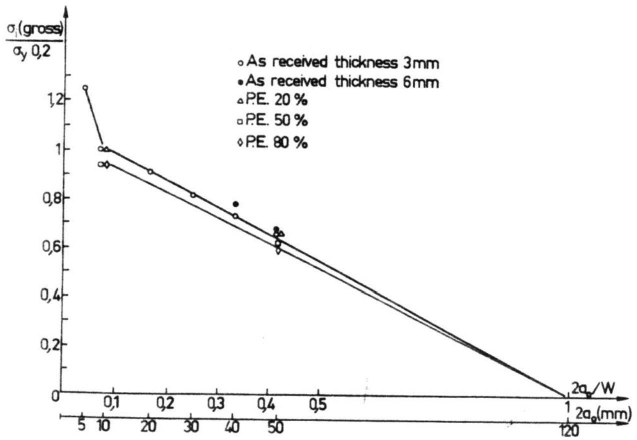

Figure 3 Center Cracked Plates. Relation Between the Gross Initiation Stress and the Crack Length

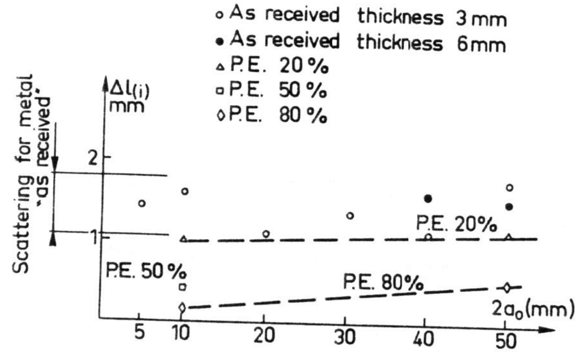

Figure 4 Center Cracked Plates. Relation Between the Central Opening and the Crack Length

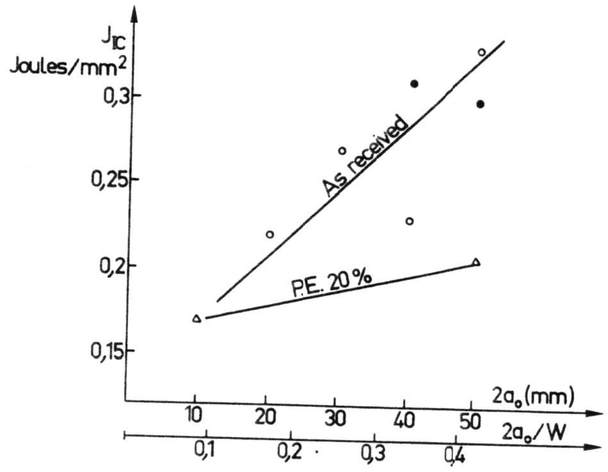

Figure 5 Center Cracked Plates. Relation Between J_{IC} and the Crack Length

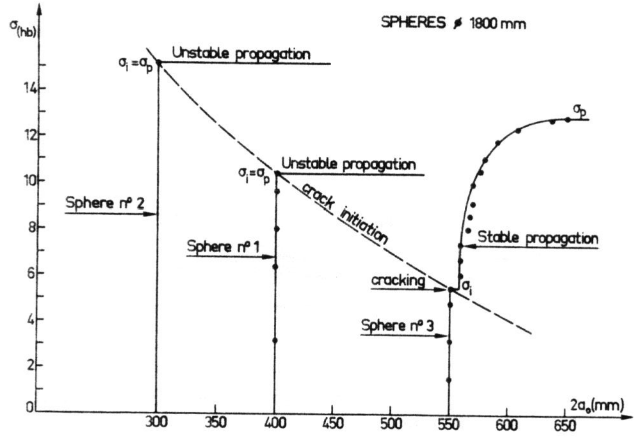

Figure 6 Spheres ∅ 1800. Curves R

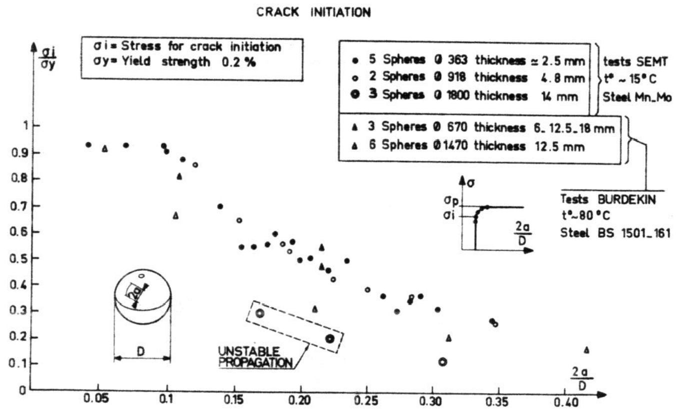

Figure 7 Spheres. Relation Between the Initiation Stress and the Crack Length

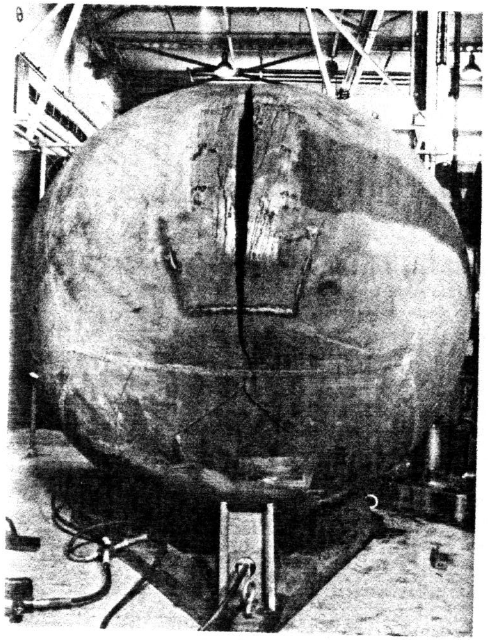

Figure 8 Sphere ∅ 1800 (n° 2) after Failure